



# Chemical characterization of mixed plastic pyrolysis oils relevant for cracker reintegration by advanced two-dimensional gas chromatography

Niklas Netsch<sup>\*</sup>, Luca Weigel, Tim Schmedding, Michael Zeller, Britta Bergfeldt, Grazyna Straczewski, Salar Tavakkol<sup>\*</sup>, Dieter Stapf

Institute for Technical Chemistry, Karlsruhe Institute of Technology, Kaiserstraße 12, 76131 Karlsruhe, Germany

## ARTICLE INFO

### Keywords:

Chemical recycling  
Plastic pyrolysis  
Thermoplastics  
Pyrolysis oil  
Two-dimensional gas chromatography  
GC×GC  
NMR

## ABSTRACT

Pyrolysis oils are the crucial link between waste and chemicals in plastic recycling via pyrolysis. Oils from mixed plastic waste pyrolysis are complex mixtures of organic compounds typically containing impurities of nitrogen, oxygen, and chlorine. Therefore, their characterization is challenging. This study presents a tailored two-dimensional gas chromatography method supporting in-depth analysis of the chemical composition. It covers a boiling range from the naphtha cut to the middle distillate. These fractions represent the preferred feedstocks to be substituted by plastic pyrolysis oils in the future. The oil characterization is complemented by elemental analyses, nuclear magnetic resonance spectroscopy, and simulated distillation. The enhanced separation by two-dimensional chromatography results in significantly higher resolution than conventional one-dimensional methods. The most relevant oil compounds can be clustered, distinguished, and quantified based on compound grouping. Depending on the boiling range of the pyrolysis oils, 77 wt% to 96 wt% of the sample composition can be elucidated. Detecting main heteroatom-containing species such as benzoic acid,  $\epsilon$ -caprolactam, acetophenone, and various aromatic nitriles provides detailed information for further pyrolysis oil utilization. The combination of the developed method with common analyses offers an advanced approach to evaluate the reintegration of contaminated mixed plastics oils into existing petrochemical value chains.

## 1. Introduction

Pyrolysis oils are essential in the pyrolytic recycling of plastic waste, linking waste management and the chemical industry in a circular economy framework [1,2]. Within this framework, chemical recycling provides complementary pathways for mechanically non-recyclable waste fractions. Fluctuating waste compositions and complex pyrolysis reaction mechanisms cause a versatile chemical composition of the pyrolysis oils [3]. This composition has a decisive influence on the feasibility of integration routes. Thus, a variety of fossil-based petrochemical product fractions can be substituted in a circular carbon economy [4]. Established petrochemical processes such as steam cracking, fluid catalytic cracking, hydrocracking, and gasification offer promising integration possibilities [5–7]. However, the properties of pyrolysis oils

must conform to fossil-based specifications of commonly used product fractions, e.g., naphtha, middle distillates, or vacuum gas oil (VGO) [8,9]. The strict specifications relate to the boiling behavior, as well as heteroatom impurities, e.g., sulfur, oxygen, nitrogen, and halogens, but also organic product components such as unsaturated hydrocarbons (HC) in the form of olefins, dienes, and aromatics [9]. However, plastic pyrolysis oils contain other compound groups in relevant quantities, extending the product spectrum to be investigated. As Kusenberg et al. conclude, comprehensive pyrolysis oil characterization requires complementary analytical methods [9]. Elemental analysis provides integral quantification of the content of carbon, hydrogen, and heteroatoms. Information on chemical structures in the pyrolysis oil, though, remains elusive [9]. This also applies, for example, to distillation or size exclusion chromatography [10,11]. Other analyses of physical and chemical

**Abbreviations:** ABS, Acrylonitrile butadiene styrene copolymer; GC×GC, Two-dimensional gas chromatography; FBP, Final boiling point; FID, Flame ionization detector; H/C, Hydrogen to carbon ratio; HC, Hydrocarbon; IBP, Initial boiling point; LDPE, Low-density polyethylene; MS, Mass spectrometer; NCD, Nitrogen chemiluminescence detector; NMR, Nuclear magnetic resonance spectroscopy; PA6, Polyamide 6; PCW, Post-consumer waste; PET, Polyethylene terephthalate; PP, Polypropylene; PS, Polystyrene; PVC, Polyvinyl chloride; SSL, Split/Splitless injector; TMS, Tetramethylsilane; VGO, Vacuum gas oil.

<sup>\*</sup> Corresponding authors.

**E-mail addresses:** [Niklas.Netsch@kit.edu](mailto:Niklas.Netsch@kit.edu) (N. Netsch), [Michael.Zeller@kit.edu](mailto:Michael.Zeller@kit.edu) (M. Zeller), [Britta.Bergfeldt@kit.edu](mailto:Britta.Bergfeldt@kit.edu) (B. Bergfeldt), [Grazyna.Straczewski@kit.edu](mailto:Grazyna.Straczewski@kit.edu) (G. Straczewski), [Salar.Tavakkol@kit.edu](mailto:Salar.Tavakkol@kit.edu) (S. Tavakkol), [Dieter.Stapf@kit.edu](mailto:Dieter.Stapf@kit.edu) (D. Stapf).

<https://doi.org/10.1016/j.fuproc.2025.108359>

Received 9 September 2025; Received in revised form 19 October 2025; Accepted 30 October 2025

Available online 14 November 2025

0378-3820/© 2025 The Authors. Published by Elsevier B.V. This is an open access article under the CC BY license (<http://creativecommons.org/licenses/by/4.0/>).

properties, such as viscosity, density, ignition temperature, calorific value, and flash point, tend to play a subordinate role in the reintegration, as their relevance is mainly focused on certain technical applications [2].

Comprehensive spectroscopic and chromatographic analysis methods are therefore essential for structural information. Proton and carbon nuclear magnetic resonance spectroscopy (NMR) [12,13] and infrared spectroscopy [14,15] are often used to determine the chemical structure of pyrolysis products. They enable the integral identification and quantification of bond types occurring in the pyrolysis samples. This allows the detection of heteroatomic bonds and the differentiation between aromatic, paraffinic, or olefinic constitution. Potential applications include quality control based on product fingerprint comparisons, as shown by Diehl and Randel for diesel and gasoline [16]. However, the complexity and variety of chemical structures in pyrolysis oils, however, is higher than in diesel or gasoline fractions. This often impedes the identification of specific compounds in the mixture. Chromatographic techniques enable this determination. They are frequently performed as gas chromatography in combination with mass spectrometers (MS) or flame ionization detectors (FID). An MS setup is used in multiple studies for the identification of unknown compounds in the pyrolysis oil to optimize the pyrolysis process [17–20]. A FID setup allows for the quantification of main components in the pyrolysis oils, which is needed to evaluate chemical recycling pathways or optimize process parameters [21,22]. The complex matrix of the pyrolysis oils often causes co-elution, resulting in uncertainties that can be eliminated by the improved separation performance of two-dimensional gas chromatography (GC×GC) [23]. In addition, GC×GC enables a group-based evaluation of the chemical composition [9]. These advantages have already been successfully demonstrated for fossil-based petrochemical products, for example, polyaromatic HCs, crude oil fractions, VGO, or light and middle distillate [24–27]. The combination of a time-of-flight MS with a GC×GC setup can significantly enhance the characterization of pyrolysis oil derived from biomass [28]. In recent years, various GC×GC configurations were developed as advanced analytical options for plastic pyrolysis oil analysis. In high-temperature GC×GC, metallic columns are used, which allow resolution of the range of high-boiling waxes of polyethylene-based oils up to C<sub>75</sub> [29–32]. Most GC×GC applications are tailored to naphtha and middle distillate ranges (C<sub>5</sub> to approx. C<sub>35</sub>) by implementing fused-silica columns for less wax-forming plastics [15,33–37]. In addition to FID and MS, GC×GC, coupled to sulfur or nitrogen chemiluminescence detectors (NCD), is popular to investigate corresponding heteroatom-containing HCs [32,34,38]. To gain qualitative information, investigations were performed for chlorinated HCs by high-resolution GC×GC–MS [39]. The application of micro pyrolyzers coupled to GC×GC for studies on the thermal degradation behavior of pure plastics and plastic waste is also established [23,40,41].

However, the reported methods focus on classifying paraffins, isoparaffins, olefins, naphthenes, and aromatics (PIONA analysis) for narrow distillation cuts, for example, pyrolysis oil-derived naphtha or gasoline [34]. HCs containing heteroatoms are usually not covered or are only detected using complementary GC×GC analyses with element-specific detectors. Simplifying the calibration effort, the quantification of different oil components is performed on the principle of equal response factors. The structural differences between and within the compound groups comprised in the pyrolysis oil are expected to cause relevant deviations in the response factors. Using the conversion factors derived from only few specific standards may lead to systematic discrimination.

Therefore, this study presents a method on an advanced GC×GC–FID–MS–NCD system for the analysis of pyrolysis oils from different thermoplastic feedstocks. The comprehensive GC×GC technique performed in a single GC setup distinguishes heteroatom-containing functional groups and various condensed and non-condensed aromatic structures of aliphatic HCs in pyrolysis oils. This method is therefore an important supplement to common PIONA analyses, which focus on aromatic and

aliphatic components rather than resolving all constituents in contaminated pyrolysis oils. This enables the identification and quantification of paraffinic, aromatic, and heteroatom-containing components in the relevant naphtha and middle distillate cut range from C<sub>6</sub> to C<sub>35</sub>. Additionally, comprehensive calibration of the main compounds and various representatives of all identified product groups is performed. Alongside the evaluation of the main products, this allows for a reliable compound group-based evaluation without the need to combine several element-specific methods. The GC×GC method was applied to various plastic-based pyrolysis oils, representing a broad spectrum of different compositions of mixed plastic waste. These oils were obtained from experiments already reported by Netsch et al. and conducted on a pilot-scale screw reactor with various pure thermoplastics, their blends, and post-consumer waste [42]. The results are evaluated considering additional elemental analyses, simulated distillation, and low-field NMR.

## 2. Materials and methods

### 2.1. Pyrolysis oil

This study examines various plastic pyrolysis oils to reflect the varying oil compositions. The investigated pyrolysis oils were obtained from a screw pyrolysis reactor at a reactor temperature of 500 °C. The electrically heated reactor was operated continuously with a feedstock addition of 1 kg/h in a nitrogen atmosphere for an experimental duration of 5 h. The feedstock residence time in the reactor was set to 30 min, ensuring complete conversion. The evolving volatiles exhibited a minimal gas residence time of about 40 s in the hot reactor zone. The gas residence time of molecules varied considerably, with a distribution width of around 300 s. The oils were separated from the permanent gas in a two-stage condensation unit after leaving the reactor. The stages were heated to 60 °C and cooled to 0 °C, respectively. The oils from both condensation stages were then reunited to obtain a representative full-range pyrolysis oil from the corresponding experiment. These full-range pyrolysis oils served as the basis for the performed analyses in this study.

Low-density polyethylene (LDPE), polypropylene (PP), and polystyrene (PS) were pyrolyzed. Additional pyrolysis oils derived from thermoplastic reference mixtures were analyzed. Oil obtained from the pyrolysis of a heteroatom-free mixture (Mix 1) comprised of 40 wt% LDPE, 30 wt% PP, and 30 wt% PS. Furthermore, pyrolysis oils from heteroatom-containing reference mixtures (Mix 2 and Mix 3) were investigated. These mixtures contained various amounts of polyethylene terephthalate (PET), acrylonitrile butadiene styrene copolymer (ABS), polyamide 6 (PA6), and polyvinyl chloride (PVC). Thus, Mix 2 and Mix 3 represent purely thermoplastic waste fractions with varying degrees of contamination covering the most important heteroatom-containing impurities such as oxygen, nitrogen, and chlorine. Moreover, the composition of a mixed thermoplastics pyrolysis oil from post-consumer waste (PCW) collection, similar to Mix 3, was examined. This waste comprises real products and contains potential additives like fillers, plasticizers, stabilizers, or flame retardants. The detailed feedstock composition of the mixtures is summarized in Table 2. Depending on the feedstock-specific condensate yield, between 2.4 and 4.4 kg of pyrolysis oil was produced per experiment. At least two tests were carried out for each input material. To rule out the influence of artifacts from previous tests, the condensate from the second test was analyzed. Further insights on experimental conditions, used feedstocks, and pyrolysis results are reported elsewhere [42].

### 2.2. Two-dimensional gas chromatography

A quantitative GC×GC–MS–FID–NCD method was developed. Quantification of main components and compound groups in the pyrolysis oils was performed with this method.

### 2.2.1. Hardware setup

The GC×GC system comprises an Agilent Technologies 8890 GC, a 5977B quadrupole MS, and an 8255 NCD. The NCD is installed in combination with an upstream FID. The setup has previously been used for qualitative analysis of pyrolysis oils from waste of electrical and electronic equipment [43] and was modified for the quantitative oil characterization. Fig. 1 shows a schematic diagram of the main components of the GC×GC system.

The split/splitless inlet (SSL) enables controlled evaporation of the injected sample at a constant temperature of 350 °C. The sample was injected into the SSL via an Agilent 7693A automatic liquid sampler. The inlet pressure was set to 34.9 PSI. The sample was introduced into the first column in split mode at a split ratio of 20:1. Helium was used as the carrier gas. The non-polar Restek Rxi-5Sil MS column with a length of 20 m, an inner diameter of 0.18 mm, and a film thickness of 0.18 µm performed the main separation. This column features a 1,4-bis(dimethylsiloxy)phenylene dimethylpolysiloxane phase. The resulting column flow rate was 0.5 mL/min. The analytes exiting the first column were transferred to the reversed flow modulator. The modulator alternates between a 10-s modulation period and a 0.36-s injection period. The analytes leaving the modulator were directed into the second separation column. A Trajan SGE BPX50 with a length of 5 m, an inner diameter of 0.25 mm, and a film thickness of 0.25 µm was used as the second column. This column is coated with a phenyl polysilphenylene-siloxane phase. The mid-polar column features a significantly higher column flow of 21 mL/min than the first column. Finally, the analytes were divided by a Trajan SilFlow GC 3-port splitter. This enabled the analytes to be introduced into the MS and the FID/NCD in a volume flow ratio of 1 to 10. The columns, the modulator, and the splitter are located in the oven. The oven was heated to 40 °C with a holding time of 3 min at the start of the measurement. This was followed by heating to the maximum oven temperature of 315 °C at a constant heating rate of 3.5 K/min. The temperature program ends after an isothermal holding period at 315 °C for 39 min. The FID was heated to 350 °C. The NCD had a base temperature of 350 °C and a burner temperature of 700 °C. The NCD was run at a pressure of approx. 3 PSI. Both detectors were operated at a data rate of 100 Hz. The MS was connected to the three-way splitter via a 280 °C transfer line. The MS ion source and the quadrupole filter were heated to 230 °C and 150 °C, respectively. The MS operated in scan mode with a scan speed of 12,500 u/s in a mass range of 30 to 300 u. This resulted in a cycle time of approximately. 40 ms. All device components and analysis parameters are summarized in Table 1.

### 2.2.2. Sample preparation and calibration

The samples were dissolved in chloroform before injection. This involved adding 1 mL of sample per 10 mL of solution. The sample mass was weighed. The concentration of the pyrolysis oils depended on the oil density and ranged between 70 and 100 mg/mL. A sample volume of 1 µL was injected. The injection syringe was cleaned with solvent before and after each injection.

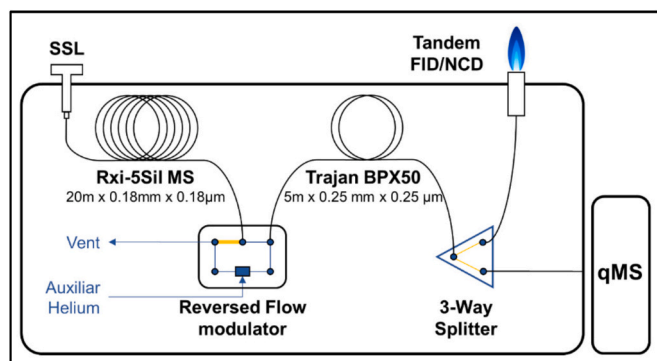


Fig. 1. Schematic overview of the employed GC×GC system.

Table 1

Overview on the hardware setup and the analysis parameters of the GC×GC method.

<b>Split/Splitless Inlet</b>			
Split mode (20:1)			
Injection with Agilent 7693A Automated Liquid Sampler	350 °C	32.94 PSI	Split flow 10 mL/min Purge flow 3 mL/min
<b>Agilent 8890 GC oven</b>			
Program: 40 °C for 3 min 40 to 315 °C at 3.5 K/min 315 °C for 39 min	First column: Rxi-5Sil MS (20 m, 0.18 mm, 0.18 µm) 0.5 mL/min	Second column: SGE Trajan BPX50 (5 m, 0.25 mm, 0.25 µm) 21 mL/min	
<b>Agilent Reversed Flow Modulator and Trajan SilFlow 3-port Splitter</b>			
Modulation period 10.0 s Modulation delay 0.01 min	Injection time 0.36 s	Split ratio (FID/NCD to MS) Approx. 10:1	
<b>FID</b>			
Data rate 100 Hz	350 °C	Air flow 400 mL/min Hydrogen flow 35 mL/min Makeup flow 20 mL/min (He)	
<b>Agilent 8255 NCD</b>			
Data rate 100 Hz	Base 350 °C Burner 700 °C	3 PSI	Oxidizer flow 8 mL/min Generator flow 37 mL/min (O <sub>3</sub> )
<b>Agilent 5977B Quadrupole MS</b>			
Scan mode: Range 30–300 u Scan speed 12,500 u/s Cycle time 40 ms	Transfer line 280 °C Ion source 230 °C Quadrupole 150 °C	Turbo pump vacuum not monitored	

Overall, 79 standards were calibrated. The calibration mixtures were prepared as a master batch of 10 mg/mL per standard in chloroform and then diluted to different concentrations. This allowed a five-point calibration with concentrations of 1.0, 2.5, 5.0, 7.5, and 10.0 mg/mL. As higher concentrations of styrene are expected in the analyzed samples, an additional calibration for high levels (10 to 70 mg/mL) was performed for this compound. An overview of the calibration mixtures and the included standards can be found in the supplementary information S1. Calibration curves were determined considering the zero point and all concentration levels. In GC×GC, blobs represent the peaks known from one-dimensional gas chromatography and can be quantified by their volume, which is proportional to the analyte mass. The concentration  $c_i$  of a component  $i$  in the pyrolysis oil was calculated using the component-specific response factor  $R_i$  and the blob volume measured in the sample  $V_i$  according to Formula 1.

$$c_i = \frac{V_i}{R_i} \quad (1)$$

The coefficient of determination was used as a criterion to assess the accuracy of the calibration lines. This coefficient was mostly higher than 0.995 except for hexylamine (0.993), benzoic acid, and some halogen-containing HCs. The determined response factors and the coefficient of determination of the calibration curves are included in the supplementary information S1. The response factor of compound groups was defined based on the individual response factor of the standards of the corresponding compound group. Supplementary information S2 contains the compound groups and their assumed response factors.

### 2.2.3. Data processing

The raw data from the GC×GC was analyzed using GC Image version 2021r3. The preprocessed FID data was converted into final quantitative results, conducting a customized VBA macro routine in MS Excel. The raw data processing included a phase shift of  $-3.1$  s and a baseline correction. The phase shift corrected the time delay effects. Automatic peak integration and data smoothing were performed in hybrid detection mode to determine the blob volumes. Blobs with a minimum intensity of 100 and a signal-to-noise ratio of less than 450 were filtered out. The blobs were then matched with the standards known from the calibration using the retention times on the first and second dimensions. In addition, all blob volumes in predefined regions of the two-dimensional chromatogram were accumulated. These accumulated blob volumes were assigned to the respective compound groups defined in a template based on the retention times. Finally, the processed data was exported as a summary report. The summary report contains all identifiable and unidentified blobs including their retention times and blob volumes. The volumes of the defined compound groups are also listed. An Excel macro calculated the mass fractions of the identified components in the sample, considering the individual pyrolysis oil concentration in each sample. For this, the identified components were compared with the calibration database. Corresponding response factors were assigned. In addition, the correctness of the assignment was checked by verifying the retention times of the standard and the component to be quantified. The compound groups were calculated similarly. This involved linking the accumulated blob volumes of regions with the assumed response factors of the compound groups. To minimize errors in the group evaluation caused by varying response factors within the group, volumes of already identified and quantified blobs were subtracted from the group volume. The residual group volume consisted solely of the volumes of unidentified blobs within the respective retention window. This residual volume was then used to calculate the residual mass of the group, applying the corresponding group response factor. Finally, the masses of the components previously determined individually were added to the respective groups. The sum of quantified compounds was then calculated.

For qualitative evaluations, MS and NCD data were processed using a baseline correction and a phase shift. In MS, the phase shift accounted  $-0.5$  s. It varies from the FID phase shift because of the differing connector geometries of the splitter and the detectors. The peaks were integrated and then identified by comparing their spectrum with the NIST20 database. This enables the identification of the main components that had not been assigned by FID retention time comparison with calibration standards. Comparing the retention times of blobs in NCD and FID data supports and simplifies the identification of nitrogen-containing compounds.

### 2.3. Further analysis methods

Elemental analyses were performed with a LECO Truspec CHN Micro elemental analyzer according to DIN EN 15104 to determine the carbon, hydrogen, and nitrogen content. A combustion ion chromatography analyzer consisting of an AQF-2100 combustion system with an Aquion ion chromatograph from a1-environsciences GmbH and Thermo Fisher Scientific GmbH was used for the determination of the chlorine content. The calorific value of the oils was measured using a C5000 calorimeter from IKA GmbH & Co. KG following DIN 51900.

Simulated distillation was performed according to ASTM D 7169:2020 in a high-temperature setup. It provides information on the product distribution of the pyrolysis oils based on the boiling curve. The analyses were carried out at a gas chromatograph equipped with a polydimethylsiloxane column. The oven program starts at  $40$  °C and ends at  $435$  °C. Analogous to the oven program, the Inlet is heated from  $50$  °C to  $425$  °C with a heating rate of  $15$  K/min. Calibration was performed with a Polywax standard mix, which was extended by short-chain n-paraffins. The samples were dissolved in carbon disulfide to a

concentration of about  $10$  mg/g.

Additional NMR analyses were performed using a Magritek Spin-solve MultiX benchtop NMR. The pyrolysis oils were investigated by  $^1\text{H}$ -NMR experiments with an  $80$  MHz permanent magnet. A sample volume of  $430$   $\mu\text{L}$  was measured three times with 16 scans and a repetition time of  $15$  s at a pulse angle of  $90^\circ$  with activated  $^{13}\text{C}$  decoupling. Chemical shift referencing was performed by adding  $20$   $\mu\text{L}$  of tetramethylsilane (TMS) before analyzing. This method allows for quantitative differentiation between protons bound in saturated and unsaturated aliphatic groups, aromatics, or heteroatom-containing functional groups. Data processing includes TMS-referencing and polynomial baseline correction. In case of LDPE pyrolysis oil, the wax-like product was analyzed after being dissolved in deuterated chloroform.

## 3. Results and discussion

### 3.1. Elemental analysis

The results of the elemental analysis are shown in Table 2. As expected, the pyrolysis oils from LDPE, PP, PS, and Mix A contain only carbon and hydrogen. The molar hydrogen to carbon ratio (H/C) in the LDPE and PP pyrolysis oils is around 2.0, indicating a paraffinic nature of the samples. Conversely, the H/C of approx. 1.1 in PS pyrolysis oil strongly hints at a predominant presence of aromatic structures.

The pyrolysis oil obtained from Mix 1 falls between these values, showing the dependence of the elemental composition on the feedstocks' polymer composition. In Mix 3, the higher share of PA6 and ABS leads to a higher nitrogen content in the pyrolysis oil. The elevated proportions of oxygen and chlorine compared to Mix 2 are caused by the higher fractions of PET, PA6, and PVC in the feedstock. The PCW has a similar elemental composition to Mix 3. Both feedstock mixtures include high amounts of polyethylene, 46.5 % and 50 %, respectively. Nevertheless, the share of PP is significantly higher in the PCW with 17.1 %, while the PS content is lower with only 3.8 %. This leads to a slightly higher H/C while the oxygen and nitrogen content remain almost unaffected. Although the proportion of PVC in the PCW is 4 % compared to 5 % in Mix 3, the chlorine content is about 0.3 % higher in Mix 3. A cause for this may be found in measurement uncertainties, but this result is to be further validated by complementary analyses. The elemental analysis reveals the strong influence of the feedstock on the oil composition. The results confirm the findings of Kusenberget al. on the importance of pyrolysis oil upgrading for subsequent processing steps in the recycling loop [9]. For example, reducing PVC in the feedstock to a practically

**Table 2**

Elemental Analysis, H/C, and the calorific value of the pyrolysis oils obtained from experiments with different plastic feedstocks in a screw reactor reported by Netsch et al. [42].

Feedstock	Elemental composition in wt%					H/C in mol/mol	Calorific value in MJ/kg
	C	H	N	Cl	O <sup>*</sup>		
LDPE	86.0	14.0	< 0.2	0.0	0.0	2.0	46.1
PP	86.4	13.6	< 0.2	0.0	0.0	1.9	45.8
PS	91.9	8.1	< 0.2	0.0	0.0	1.1	41.4
Mix 1 <sup>A</sup>	88.6	11.4	< 0.2	0.0	0.0	1.5	44.0
Mix 2 <sup>B</sup>	86.3	13.1	< 0.2	0.2	0.4	1.8	45.2
Mix 3 <sup>C</sup>	86.3	11.7	0.6	0.5	0.9	1.6	43.5
PCW <sup>D</sup>	85.9	12.5	0.5	0.2	0.9	1.7	44.3

<sup>\*</sup> Calculated as the difference to 100 %.

<sup>A</sup> Contains 40 % LDPE, 30 % PP, 30 % PS.

<sup>B</sup> Contains 70 % LDPE, 20 % PP, 4 % PET, 2 % PS, 2 % PA6, 2 % PVC.

<sup>C</sup> Contains 50 % LDPE, 15 % PP, 10 % PET, 10 % PS, 5 % ABS, 5 % PA6, 5 % PVC.

<sup>D</sup> Contains 29.4 % LDPE, 25.1 % PP, 17.1 % HDPE, 10.1 % PET, 6.3 % PA6, 4.2 % PS, 4.0 % PVC, and 3.8 % ABS.



undetectable content in realistic applications is required to achieve the chlorine content in oils approaching the specification limit of 3 ppm. Also, the product upgrading, for example in the form of hydrotreating, is crucial for nitrogen and oxygen compounds, as the limit of 100 ppm is exceeded by far in elemental composition.

### 3.2. Simulated distillation

The simulated distillation results are displayed in Fig. 2 along with the boiling ranges of the common petrochemical products naphtha, middle distillate, and VGO. Supplementary information S3 contains a list of determined shares of these boiling ranges for all pyrolysis oils.

All pyrolysis oils feature a distillation curve over a broad temperature range. These are characterized by the initial (IBP) and final boiling points (FBP). Both characteristic parameters differ slightly depending on the pyrolysis feedstock. PP oil exhibits the lowest IBP of about 50 °C, while PS has the highest at 103 °C. The FBP for all oil ranges from 545 °C (Mix 1) to 601 °C (Mix 3). The wide boiling range indicates the products' significantly broad molecular weight distribution. The LDPE pyrolysis oil reveals the smoothest curve, and thus the most even distribution across the various boiling cuts, which agrees with previously published results [29,44]. The boiling range up to 200 °C, corresponding to a naphtha cut, dominates the composition of all oils. The pyrolysis oil of LDPE exhibits the lowest content of naphtha at 41 wt%. PS, with its styrene-selective decomposition mechanism, contains the highest proportion of compounds in the naphtha range at 75 wt%, similar to Mix 1. Horizontal segments are recognizable in the PS and Mix 1 distillation curve. These segments indicate an increased concentration of certain components, presumably styrene and its oligomers, in the pyrolysis oil. The middle distillate and the VGO section are similar in all pyrolysis oils. The pyrolysis oils of the reference mixtures and the PCW behave similarly to LDPE, resulting from the high proportion of polyethylene in the feedstocks. With lower contents of PE in the feedstock, the curve shifts towards lower boiling ranges and therefore the naphtha and middle distillate cuts. However, mechanically non-recyclable waste fractions that appear promising for chemical recycling via pyrolysis mainly contain high polyethylene content. Therefore, pyrolysis processes must deal with such feedstocks. By optimizing reactor design and process parameters, the boiling range can be adjusted. For example, higher temperature in the pyrolysis of polyethylene shifts the product composition towards low-boiling compounds as reported in several studies [1]. Nevertheless, no pronounced horizontal lines are visible in den mixed

plastics pyrolysis oils, which indicates a broad product composition. Consequently, the oil of these feedstocks is not favorable for extracting specific base chemicals, as seen for the PS oil with its potential high styrene concentration. An in-depth analysis of the pyrolysis oil components is essential to further investigate the chemical structure of compounds incorporated in the oil. Therefore, NMR and GC×GC analysis are crucial.

### 3.3. Low-field NMR analysis

The results obtained from the NMR measurements of the pyrolysis oils allow qualitative comparison with the GC×GC analyses. They offer the advantage of analyzing the entire sample without limitations of physical properties, like the boiling behavior. The  $^1\text{H}$ -spectra of the pyrolysis oils from LDPE, PP, PS, and PCW are shown in Fig. 3. The spectra of the reference mixtures are given in supplementary information S4. Different functional groups of the contained molecules were identified in the labeled chemical shift regions [45]. The peak integration in these regions allows a quantitative assessment of the  $^1\text{H}$ -nuclei content of the respective groups. This enables a quantitative comparison of the pyrolysis oil composition. Additionally, Table 3 lists the entire quantitative results.

The LDPE and PP pyrolysis oils contain dominant signal intensities in the aliphatic range. The difference between the samples relates to the distribution of  $\text{CH}$ -,  $\text{CH}_2$ -, and  $\text{CH}_3$ -groups. While the proportion of  $\text{CH}_2$ -groups prevails in LDPE, PP pyrolysis oil mainly contains  $\text{CH}$ - and  $\text{CH}_3$ -groups. This demonstrates the difference in the decomposition behavior of the two polyolefins. While LDPE is known for its mainly long-chain unbranched  $n$ -alkanes,  $\alpha$ -olefins, and  $\alpha$ - $\omega$ -dienes, PP pyrolysis produces mainly branched saturated and unsaturated aliphatics [44]. The less frequently detected olefinic-bound protons confirm these findings in both pyrolysis oils. In PS oil, however, mainly aromatically bound protons are detected, representing the known product distribution of styrene, its oligomers, and other monoaromatic molecules [46]. The aliphatic and olefinic proton intensities are caused by substituents on aromatic compounds. After pyrolyzing the mixture of these polymers, Mix 1, aromatics, and various aliphatics are detected in the oil sample as expected.

In the pyrolysis oils of the other thermoplastic reference mixtures and the PCW, protons in carbonyl and carboxyl groups can be identified. However, the peaks are comparably weak because of the small number of protons bound in products with these functional groups. These molecules might form during pyrolysis, originating from PET degradation into benzoic acid or terephthalic acid [47]. The higher the PET content in the sample, the more pronounced the peak in this chemical shift range. Aliphatic components have the highest intensity in these samples as well. The proportion of protons in the range of 3.5 to 4.3 ppm is increased compared to LDPE, PP, PS, and Mix 1. This indicates an increased proportion of protons in the  $\beta$ -position to nitrogen-, chlorine-, or oxygen-containing groups [45]. The proportion of aromatic structures increases successively with the addition of PS, ABS, PET, and PVC, which is in line with the decomposition products of the pure substances. In addition to PS and PET, PVC also tends to form aromatic structures during pyrolysis. This primarily occurs in the final PVC pyrolysis stage of polyene chain degradation [48]. ABS polymer selectively forms styrene and other BTX aromatics [49] based on its copolymer structure, similar to PS. Thus, the proportion of aromatic structures increases successively with the addition of PS, ABS, PET, and PVC, which is consistent with reported degradation products of the pure polymers. The NMR analyses provide fast and general information that complements the elemental analysis, but lack details on the specific main compounds in the sample. Since  $^1\text{H}$ -functional groups are determined instead of the existing compound groups, the comparison with GC×GC compound group results is limited. Also, heteroatom-containing impurities in the paraffinic and aromatic matrix are resolved poorly within the spectrum because of their lower concentration and, therefore, lower signal intensity.

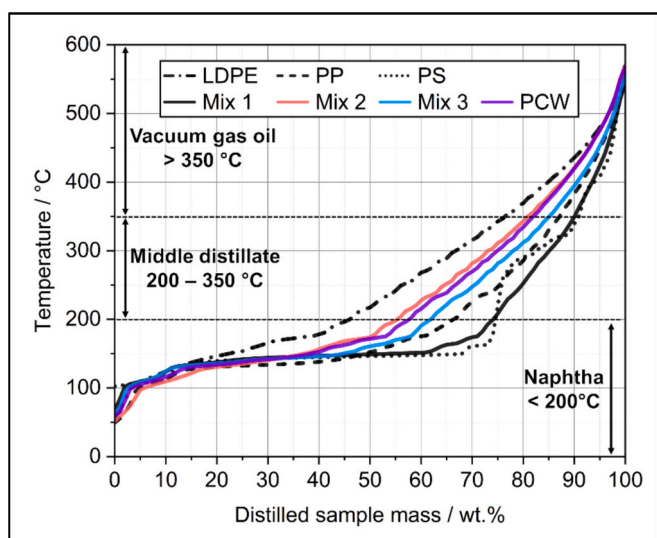


Fig. 2. Simulated distillation curve of the analyzed pyrolysis oils obtained from different thermoplastic feedstocks.

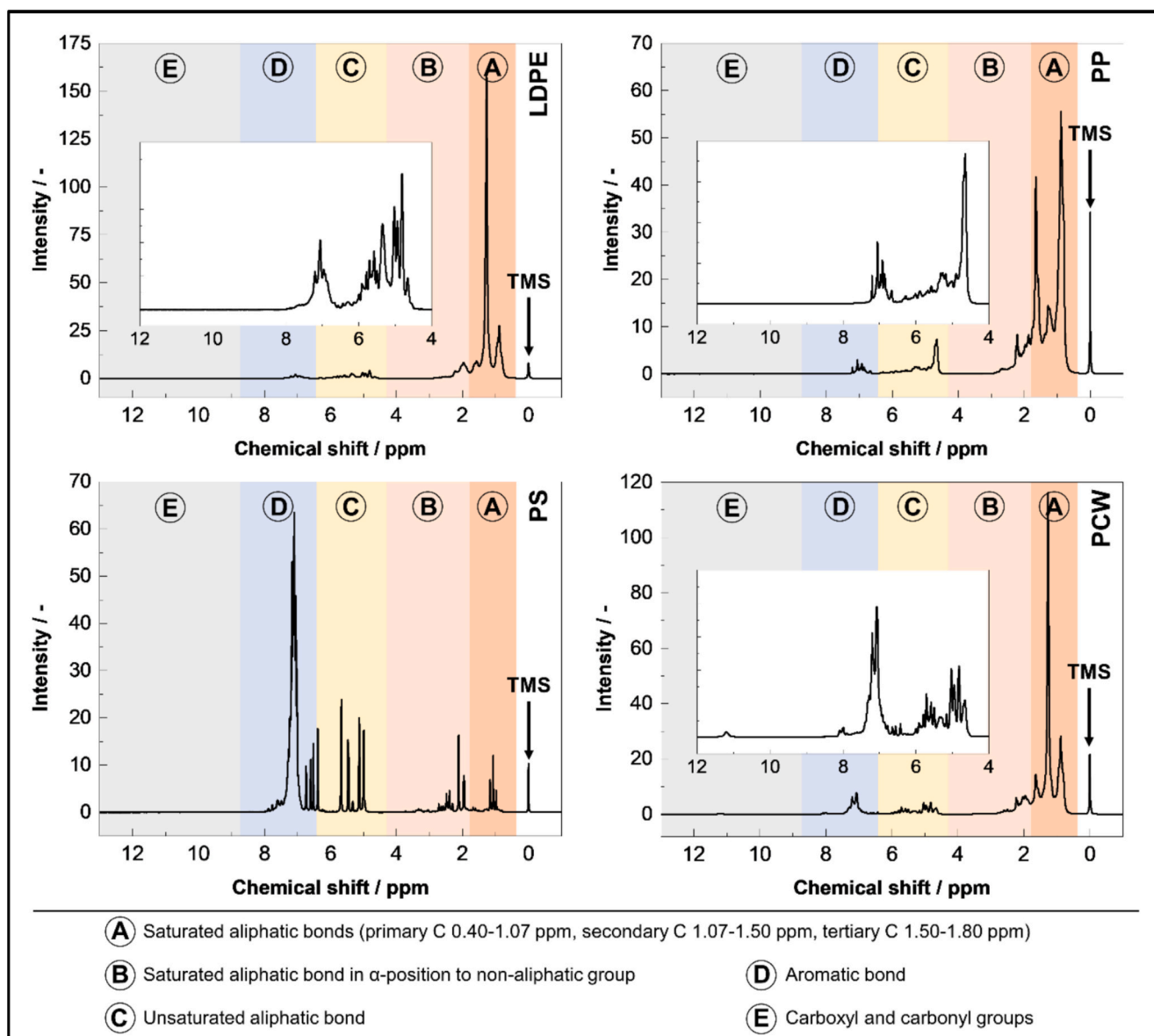


Fig. 3. Comparison of  $^1\text{H}$ -NMR spectra of LDPE, PP, PS, and PCW pyrolysis oils.

### 3.4. Two-dimensional gas chromatography

Information about the molecular structure of the pyrolysis oil components is essential for subsequent processing and recycling. Therefore, in-depth GC $\times$ GC analyses supplement the elemental analysis and NMR.

#### 3.4.1. Qualitative analysis and main compound quantification

The GC $\times$ GC chromatogram and the main components are exemplarily shown for the pyrolysis oil of LDPE, PS, and the PCW in Fig. 5, Fig. 6, and Fig. 6. Supplementary information S5 contains the chromatograms and Table S5.1, which lists the main compounds of the remaining pyrolysis oils under investigation in this study. The analytes are separated in the first dimension based on the molecular weight or boiling point of the compounds. In the second dimension, the polarity of the components is decisive. The comprehensive external calibration carried out in advance enables the quantification of a large proportion of these components.

In the pyrolysis oil of LDPE, mainly unbranched aliphatics with increasing chain length are recognized in Fig. 4 at a second-dimension retention time of about 2 s.  $\alpha$ -Olefins dominate, but the corresponding

n-alkane and  $\alpha$ - $\omega$ -diene can also be identified for each chain length. These structures form regular triplets. For the  $\text{C}_{10}$  triplet,  $\alpha$ -decene, n-decane, and  $\alpha$ - $\omega$ -decadiene with 2.1 wt%, 0.8 wt%, and 0.3 wt%, respectively, can be determined exemplarily. The proportions of triplets are almost constant and only decrease noticeably after reaching  $\text{C}_{25}$ . This decline can be attributed to the evaporation behavior of these HCs. The evaporation temperature of wax-like aliphatics exceeds the inlet temperature of the SSL. Therefore, a partial evaporation of such compounds is seen by a decreasing blob volume with increasing chain length from  $\text{C}_{25}$  upwards. Long-chain aliphatics are underestimated, which is in line with the comparatively high VGO Cut content of this pyrolysis oil. As expected, no heteroatom-containing compounds were detected. However, slightly increased levels of monoaromatics, naphthalene, and indene are recognizable. These products cannot be explained by the primary decomposition mechanism proposed by Bockhorn et al. [44]. The pyrolysis oils were generated in a pilot-scale screw pyrolysis reactor. Secondary reactions possibly cause alkyl-aromatics formation, which explains, for example, the toluene and xylene contents of 0.8 wt% each. However, styrene and  $\alpha$ -methylstyrene are not common secondary reaction products of unsaturated gases. Before the LDPE experiments, the

**Table 3**

Proton quantification according to their functional groups and corresponding chemical shift from integrated low-field NMR analysis results.

Pyrolysis oil feedstock	<sup>1</sup> H-nuclei distribution according to chemical shift ranges in % (mol/mol)						
	Saturated aliphatic bonds			<sup>1</sup> H near a nonaliphatic bond <sup>D</sup>	Unsaturated aliphatic bonds <sup>E</sup>	<sup>1</sup> H in Aromatic bond <sup>F</sup>	<sup>1</sup> H in a carboxyl or carbonyl group <sup>G</sup>
	R-CH <sub>3</sub> <sup>A</sup>	R <sub>2</sub> -CH <sub>2</sub> <sup>B</sup>	R <sub>3</sub> -CH <sup>C</sup>				
LDPE	17.6	79.0 54.4	7.0	11.4	7.0	2.6	0.0
PP	38.0	75.8 17.2	20.6	13.3	8.5	2.4	0.0
PS	2.1	5.5 2.5	0.9	9.9	15.3	69.3	0.0
Mix 1	19.1	57.6 29.4	9.0	12.1	9.9	20.4	0.0
Mix 2	19.8	73.8 44.2	9.8	12.1	9.0	5.0	0.1
Mix 3	20.3	65.7 36.6	8.8	12.6	7.9	13.6	0.2
PCW	19.6	70.2 41.0	9.6	12.5	8.3	8.7	0.3

Spectrum was integrated in specific chemical shift areas of <sup>A</sup> 0.40–1.07 ppm, <sup>B</sup> 1.07–1.50 ppm, <sup>C</sup> 1.50–1.80 ppm, <sup>D</sup> 1.80–4.30 ppm, <sup>E</sup> 4.30–6.30 ppm, <sup>F</sup> 6.30–8.70 ppm, and <sup>G</sup> 8–70–13.00 ppm.

reactor was flushed using multiple polystyrene experiments. This flushing helped clean the condensers of viscous deposits before the experimental campaign. Some components may originate from these preliminary experiments as artifacts. The styrene component accounts for a small proportion of 0.70 wt%. Such artifacts are not detected in other pyrolysis oils generated in the later experiments.

The PP pyrolysis oil consists mainly of branched aliphatics as shown in the chromatogram in the supplementary information (S5). Compared to the LDPE sample, the majority of the components are detectable in the range up to C<sub>20</sub>. The components 2,4-dimethylheptene, trimethylnonene, and isopentadecene stand out as main blobs. These are known to be primary decomposition products of PP pyrolysis [44]. A 2,4-dimethylheptene content of 7.2 wt% can be determined. The lower molecular weight of the aliphatics compared to the LDPE sample explains the results of the simulated distillation. The PP sample contains small amounts of alkyl aromatics. Only xylenes, toluene, benzene, and n-propylbenzene can be quantified. Secondary reactions of reactive gaseous components might cause their formation, since PP tends to selectively degrade into reactive compounds like propylene and other branched olefins.

In contrast to polyolefins, PS oil only contains aromatic structures, predominantly in the monoaromatic range. The chromatogram is shown in Fig. 5. The styrene monomer content is 52.5 wt%, which represents a low but reasonable value compared to other studies [46,50]. In addition, higher contents of ethylbenzene (7.1 wt%), α-methylstyrene (5.3 wt%), and toluene (4.6 wt%) are measured. Relevant quantities of diphenyls are identified, while further dimers are present in the chromatogram. The non-calibrated components, 1,2-diphenyl-isobutylene and 1,3-diphenyl-propane, are identified as main diphenyl compounds. The pronounced styrene trimer blob amounts to 0.88 wt%.

Mix 1 pyrolysis oil comprises the main components also present in LDPE, PP, and PS pyrolysis oil, but with minor intensities. The corresponding chromatogram to Mix 1 pyrolysis oil can be found in the supplementary information S5. Considerable amounts of previously unidentified structures are not detectable. Blobs in the range of retention times of 40 to 80 min and 3 to 4 s are recognizable. Monoaromatics with long-chain alkyl substituents might be found in this retention time range. However, the structures cannot be identified beyond doubt using MS because of low signal intensities. Supplementary information (S5) also contains the results for the pyrolysis oil from Mix 2. Branched and unbranched aliphatics dominate the composition of the pyrolysis oil Mix 2, as expected from the high LDPE and PP content in the feedstock. 6.2 wt% n-alkanes and 18.1 wt% α-olefins are determined in total. The

proportion of 2,4-dimethylheptene accounts for 1.5 wt%. Only a few aromatic structures are detectable. Toluene, styrene, xylenes, and benzene are present in increased quantities. Apart from styrene, these components are known from the PET and PVC product distribution reported in the literature [47,48]. The elemental analysis indicates oxygen- and chlorine-containing compounds in the oil. Benzoic acid (0.7 wt %), cyclopentanone, acetophenone, and benzaldehyde are identified as the main oxygen-carrying compounds. In addition, benzonitriles (0.2 wt %), ε-caprolactam (0.2 wt%), and ortho-toluidine are identified. These results align with the elemental analysis, which shows no nitrogen but features a detection limit of 0.2 wt% of total nitrogen in the oil sample. Using the quantified heteroatom-containing compounds in Table S5.1 of the supplementary information, a total nitrogen content of 0.06 wt% can be determined by GC×GC. The estimation relies on the respective molar masses and structural formulas of the products. Likewise, the GC×GC analysis provides an oxygen content in the oil of 0.20 wt%. A total chlorine estimation based on the GC×GC results in comparison to the elemental analysis is not feasible, as only one major compound could be specified in the pyrolysis oil of Mix 3 and the PCW with certainty. At retention times of 22 min and 5.8 s, 1-(chloroethyl)-benzene was found. Several other blobs of low intensity were identified, which might represent organochlorine HCs. For these blobs, the match factor of MS data is very low with the quadrupole MS. Wrong positive and false negative identifications of chlorinated compounds are therefore likely. This finding is also concluded by Jean et al., who investigated chlorinated HCs in pyrolysis oils using an advanced GC×GC setup [39]. They also highlight the distinct specification of chlorine compounds as challenging, even with their method specifically tailored for chlorinated compounds. Only a few organochloride structures could be ascertained by the Authors. They report significant misassignments by the algorithms.

Oxygen and chlorine content derived from the GC×GC analysis are below the values of the elemental analysis. GC×GC, therefore, provides further insights into the evaluation of low limits of heteroatom impurities in the sample. Nevertheless, blobs of heteroatom-containing components for low-boiling HCs may overlap with the solvent. Also, traces of heteroatom-containing HC structures may feature very low blob intensities. Thus, such chemical structures are not detectable, which explains the higher values of the elemental analysis. The feedstocks Mix 3 and PCW exhibit a similar plastic composition. The chromatogram depicted in Fig. 6 indicates the complex composition of the oil. Compared to Mix 2, both oils have a lower content of aliphatics, which is caused by the lower content of polyolefins in the pyrolysis

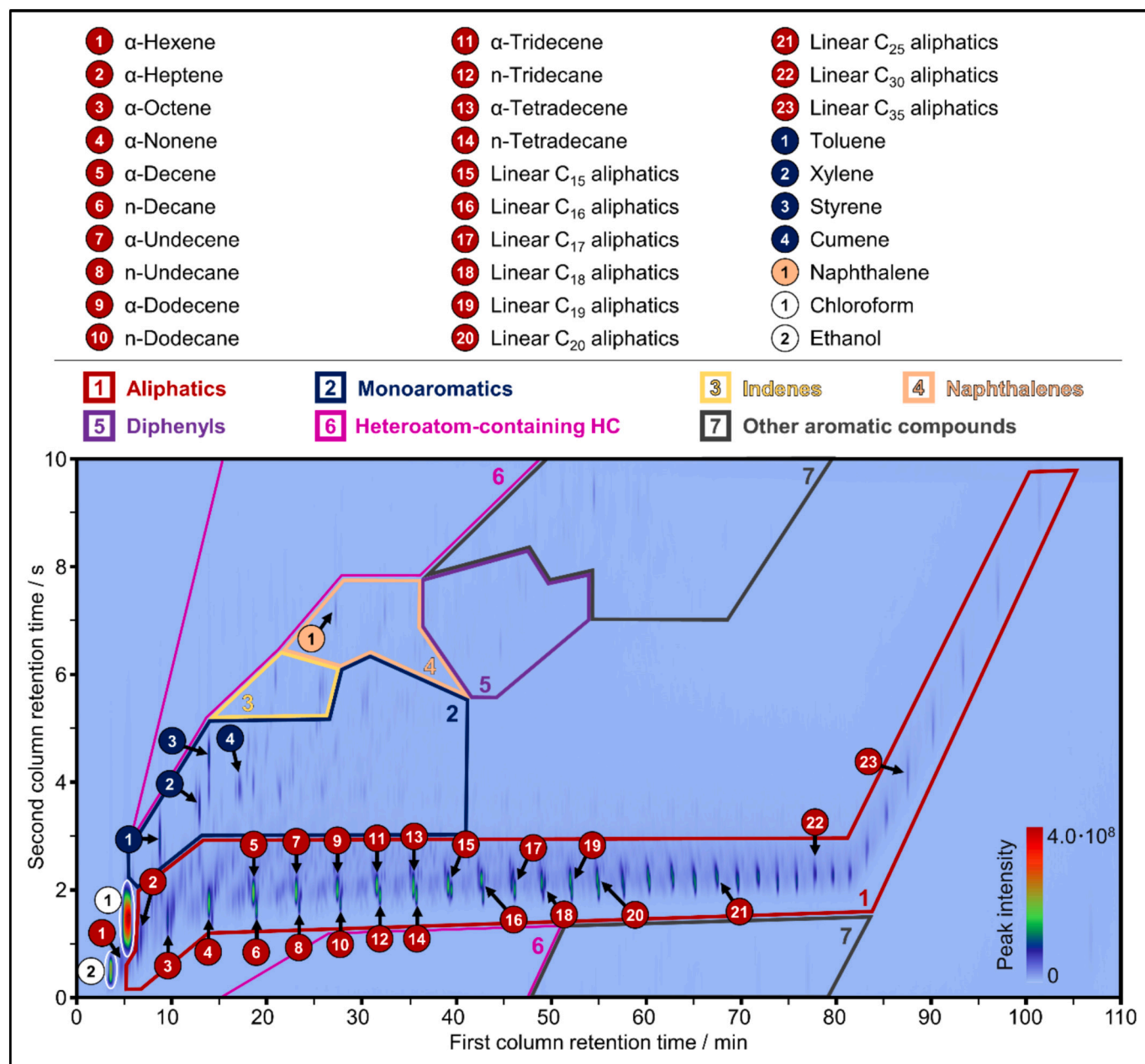


Fig. 4. GCxGC chromatogram of the LDPE pyrolysis oil analysis with labeled main compounds.

feedstock. Their feedstocks contain higher amounts of PA6, PET, PVC, PS, and ABS. In both pyrolysis oils, similar compositions can be found. However, less PS and ABS in PCW leads to a styrene content of only 3.7 wt% in PCW compared to 6.8 wt% in Mix 3. At the same time, the PP content in PCW is significantly higher. This leads to 1.9 wt% 2,4-dimethylheptene in the PCW pyrolysis oil compared to 1.0 wt% in Mix 2. The heteroatom-containing compounds already identified in the pyrolysis oil of Mix 2 are found in both mixtures. However, the proportion of benzoic acid is significantly higher in the pyrolysis oil of Mix 3 and the PCW, at 1.7 wt% and 1.5 wt%, respectively. More aromatic nitriles are also detected in the form of benzonitriles, o-toluidine, methyl benzonitrile, and 2-phenyl-butyronitrile. ε-Caprolactam appears in both pyrolysis oil samples in smaller quantities than in Mix 2, despite the higher PA6 content. The nitrogen and oxygen content, which can be estimated from the main compounds in the pyrolysis oil of the PCW, is 0.13 wt% and 0.42 wt%. For Mix 3, the contents are similar with 0.10 wt% and 0.46 wt%. These values fall below the detection limit or the respective results of

the total N and O content determined by elemental analysis. Missing calibrations of specific compounds pose a reason why not all of the identified heteroatom-containing HCs can be quantified. This applies to nitrogen in the form of methyl-benzonitrile or benzobutanenitrile, for example. However, other heteroatoms are likely also distributed among a large number of other HCs in quantities too low for identification. This assumption particularly concerns HCs that contain chlorine. Jean et al. identified up to 1800 chlorinated compounds in their experimental study [39]. Yang et al. detected various chlorine-containing light HCs and long-chain HCs in addition to chlorinated monoaromatics, such as 1-(chloroethyl)-benzene, which was also identified in this study [51]. Gui et al. describe that many polyaromatic compounds are formed during the pyrolysis of PVC [52]. In addition to monoaromatics, these condensed polyaromatics also contain one or more chlorine atoms. Additional chlorinated hydrocarbons that the primary PVC decomposition mechanism cannot explain were found to result from interactions between PVC and other polymers. Cao et al. encountered strong



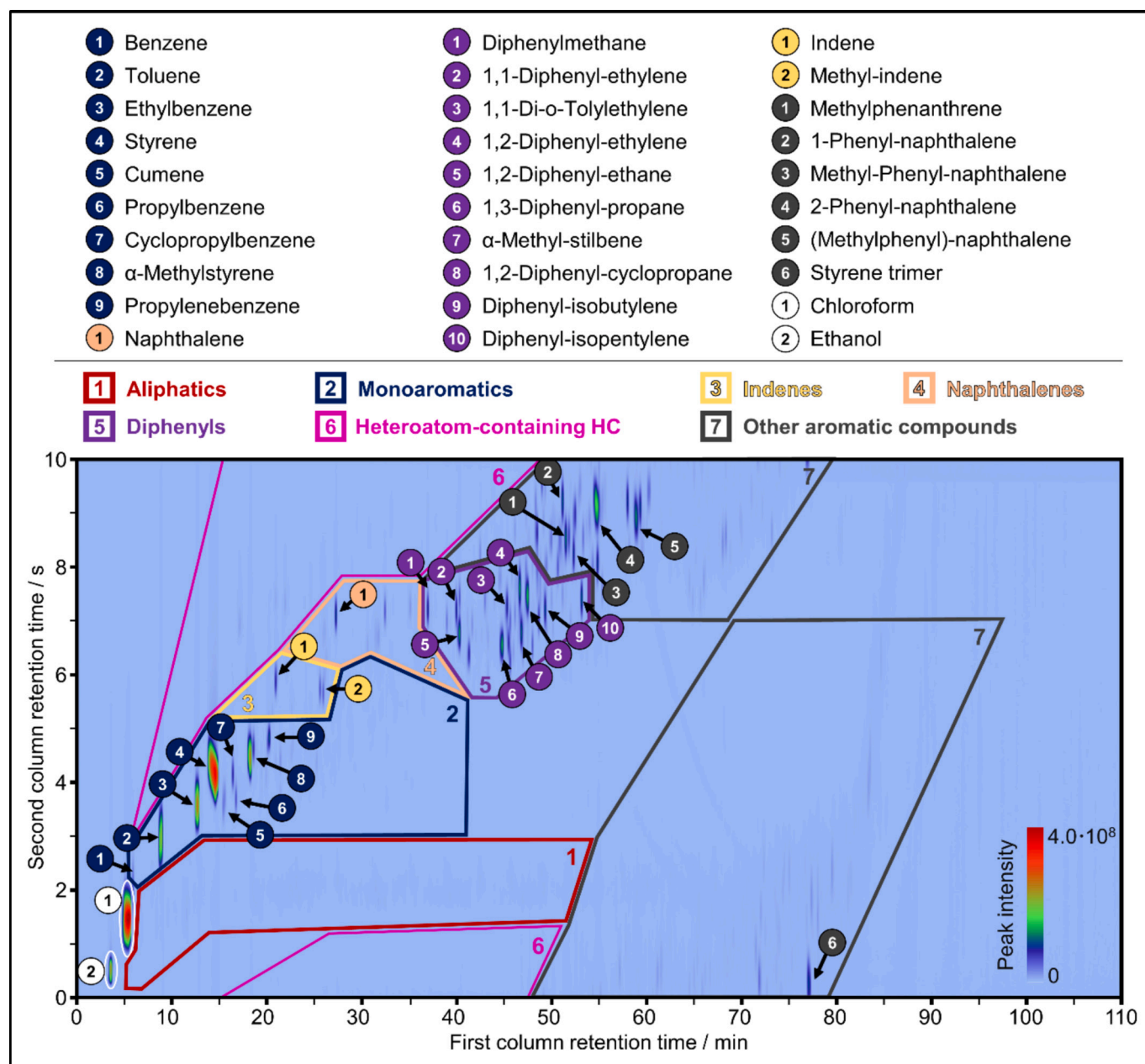


Fig. 5. GC×GC chromatogram of the PS pyrolysis oil analysis with labeled main compounds.

interactions between PVC and PET in their pyrolysis study [53]. These interactions, for example, lead to the formation of small amounts of chlorinated derivatives of terephthalic and benzoic acid. Such chlorinated terephthalic compounds fall into the temperature limitations of the GC×GC method. In general, other chemical compounds may be present in the oil that exceed the analyzable boiling range of this analytical method.

Neither cyclic nor linear silicon compounds were present in the pyrolysis oils obtained from LDPE, PP, PS, or the reference mixtures. As they are mainly introduced by additives or coatings, their absence is expected [9]. Despite the possible additives in the plastic products of the PCW, no silicone compounds were identified in this oil either.

As described above, the GC×GC parameters and operating principles set technical limits. The method allows measurements in the range from  $C_6$  to  $C_{25}$ . It therefore covers the naphtha and middle distillate range almost entirely. For longer aliphatics from  $C_{25+}$ , complete evaporation is limited due to the maximum temperature of the columns of 315 °C and

the inlet temperature of 350 °C. Maintaining the column setup because of its high separation efficiency, increasing the oven temperature would irreversibly damage the columns. Increasing the inlet temperature can cause compound degradation during injection and leads to long-term accumulation of high boilers on the column. Therefore, this represents a recognizable upper limitation. Accordingly, partial quantification of the oil sample compounds in the VGO range is concluded. A second limit of the GC×GC analysis method is the low resolution of components with low retention times in the range from  $C_6$  to  $C_7$ . For example, blob overlapping of n-hexane and  $\alpha$ -hexene occurs, leading to inaccuracies. Therefore, this blob is summarized as  $\alpha$ -hexene due to its higher expected content in the product spectrum of LDPE. Other compounds, such as cyclohexanes,  $C_5$  and  $C_6$  isoaliphatics, or short-chain heteroatom-containing structures such as acetone, chlorobutanes, butanone, or ethyl acetate, also overlap in this range. Interference with the solvent blobs of chloroform or ethanol stabilizer contained in the solvent is possible.

This hypothesis was also verified experimentally with reference

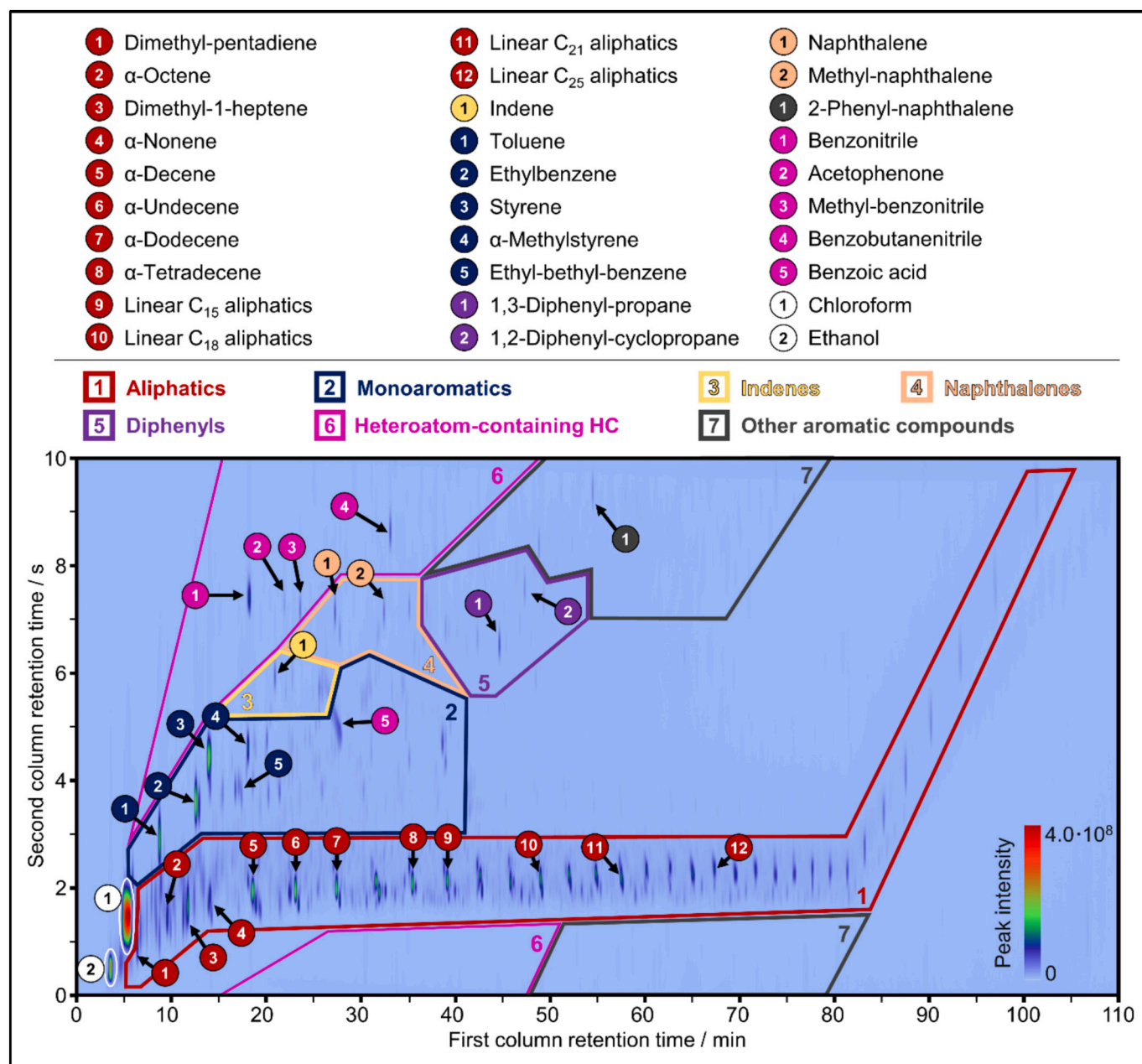


Fig. 6. GCxGC chromatogram of the PCW pyrolysis oil analysis with labeled main compounds.

standards for some of these components. The described method consequently only allows a reliable evaluation of benzene and aliphatics with a chain length of C<sub>7</sub> onwards. Furthermore, the effect concerning the second dimension may limit the analysis. Highly polar or large chemical structures, such as heteroatom-containing HCs or polycyclic aromatics, exhibit a higher retention time than monoaromatics or small-chain aliphatics. A retention time that exceeds the modulation time by far causes so-called wrap-around effects, which can inevitably represent a reason for overlapping peaks. However, this effect is only observed for a few oil components and in particular for high-boiling products due to the tailored development of the method, designed to minimize these effects. Wrap-around influence is therefore negligible. Consequently, the presented GCxGC technique allows excellent separation of complex pyrolysis oils. The strength of the method lies mainly in the separation of aromatic and aliphatic structures. The peak overlap in the study presented here is reduced to a minimum compared to one-dimensional gas chromatography. For example, the baseline-corrected evaluation of

styrene, o-xylene, and α-nonene is possible. In a one-dimensional configuration without a second column, these components feature similar retention times and would overlap, preventing reliable quantitative evaluation. With the separation in the second column, this effect is overcome. This advantage of the GCxGC configuration also applies to many other components, such as ε-caprolactam and C<sub>12</sub> aliphatics, or benzobutanenitrile and C<sub>13</sub> aliphatics.

The resolution in the aliphatic range is good enough to separate calibrated n-alkanes from α-olefins and dienes. N- and isoaliphatics, and olefins fall into a common retention time window, preventing automated evaluation of aliphatics. Thus, methods specially customized for their analysis are required, as presented by Abbas-Abadi et al. and Kusenberg et al. for polyolefins [26,29,31]. The high-temperature GCxGC method developed by the authors enables a more precise resolution of alkanes, α-olefins, and α-ω-dienes, as well as the differentiation of branched and unbranched paraffines and naphthenes. Additionally, the high-temperature adaptations also allow for the measurement of

waxes with a chain length of up to C<sub>75</sub>. However, this method accompanies a major disadvantage. It probably requires even higher modulation times for the separation of aromatics and heteroatom-containing HCs to avoid interference caused by wrap-around effects. Thus, we expect the method to be only advantageous for contamination-free, polyethylene-based pyrolysis oils. In contrast, the method presented in this study focuses on the analysis of pyrolysis oils from contaminated polyolefin-rich mixed plastics.

### 3.4.2. Quantitative compound group analysis

The quantitative analysis of the pyrolysis oil, categorized by compound group, is presented in Fig. 7. The full dataset is included in the supplementary information (Table S5.2). The method is designed so that compounds with similar chemical structures elute at similar retention times in both dimensions. This results in the accumulation of similar compounds in specific areas. Consequently, these compounds can be distinguished as compound groups quantitatively. Although aliphatic compounds cannot be differentiated by automated group evaluation, the group of aliphatics was further differentiated in more detail, considering the main compound-specific determination. As linear n-alkanes and  $\alpha$ -olefins represent a major proportion of the aliphatic group, the component-specific quantification can be implemented in the group-based evaluation. This enables the aliphatic group to be differentiated in more detail into n-alkanes (chain lengths C<sub>6</sub>–C<sub>21</sub>, C<sub>25</sub>, and C<sub>30</sub>),  $\alpha$ -olefins (chain lengths C<sub>6</sub>–C<sub>20</sub>), and other aliphatic compounds.

A strong influence of the feedstock is also evident in the group analysis. However, the group-based evaluation quantifies significant proportions of additional, non-calibrated compounds within respective compound groups. This capability constitutes the primary advantage of the novel GC $\times$ GC methodology. In contrast to most conventional one-dimensional methods, this approach captures the sample composition almost entirely. For example, paraffinic contents of 74 wt% for LDPE and 86 wt% for PP are detected. The sum of identified compounds serves as an indicator for the maximum analyzable share of pyrolysis products using the presented GC $\times$ GC method. The gap to a fully closed analysis stems primarily from the already discussed technical limitations at the boundaries of the boiling point range. Uncertainties arising from fluctuating response factors in a compound group appear to be of minor

influence. The relatively fine integration of blob volumes leads to minor errors in the group-based quantification, as seen in the heteroatom-containing HC group for LDPE, PP, and PS pyrolysis oils. However, this error can be estimated to be around 0.1 wt% in the final results.

The mass balance gap of 16 wt% in LDPE pyrolysis oil, when compared with 5 wt% for PP pyrolysis oil, is plausible considering results from simulated distillation. The highest share of the VGO cut is estimated for the LDPE sample with 33 wt%. Compounds of this cut feature a boiling point over 350 °C, which corresponds to the inlet temperature of the GC $\times$ GC system or even exceeds it. Consequently, compounds of this cut are only partly detectable in the GC $\times$ GC analysis of LDPE oil. Similarly, for PP, a VGO content of 17 wt% aligns with the compound group evaluation gap identified by GC $\times$ GC. In LDPE samples, the aromatic artifacts from cleaning cycles are also visible within the compound group results. The PS pyrolysis oil is composed predominantly of monoaromatics, diphenyls, and other aromatic compounds. The detected distributions are consistent with the data reported by Faravelli et al., indicating a composition of styrene, other monoaromatics, dimers, and trimers [46]. The low share of heteroatom-containing HCs in PS can be attributed to the tailing of the dominant styrene peak in the second dimension of the chromatogram. In Fig. 4, three low-intensity peaks are visible in this region, which are likely artifacts from previous experimental runs in the pilot plant. The pyrolysis oil from Mix 1, comprising LDPE, PP, and PS, consists of the corresponding product groups. High paraffinic and monoaromatic contents are detected. The minor content of heteroatom-containing HCs (0.4 wt %) results, analogously to PS, from the uncorrected tailing of the PS peak into this region. The pyrolysis oils from Mix 2, Mix 3, and PCW contain significant proportions of paraffinic compounds along with monoaromatics and heteroatom-containing HCs. While the results align with the main compound analysis, significantly higher levels of heteroatom-containing HCs are now detected. This confirms the prior hypothesis that additional traces of HCs with heteroatom-containing functional groups are present but not individually identifiable as discrete blobs.

These results highlight the benefit of group-based evaluation. A substantially higher proportion of the sample is characterized compared to the main compound analyses, enabling an almost complete mass balance of the composition. Associated uncertainties are also estimable.

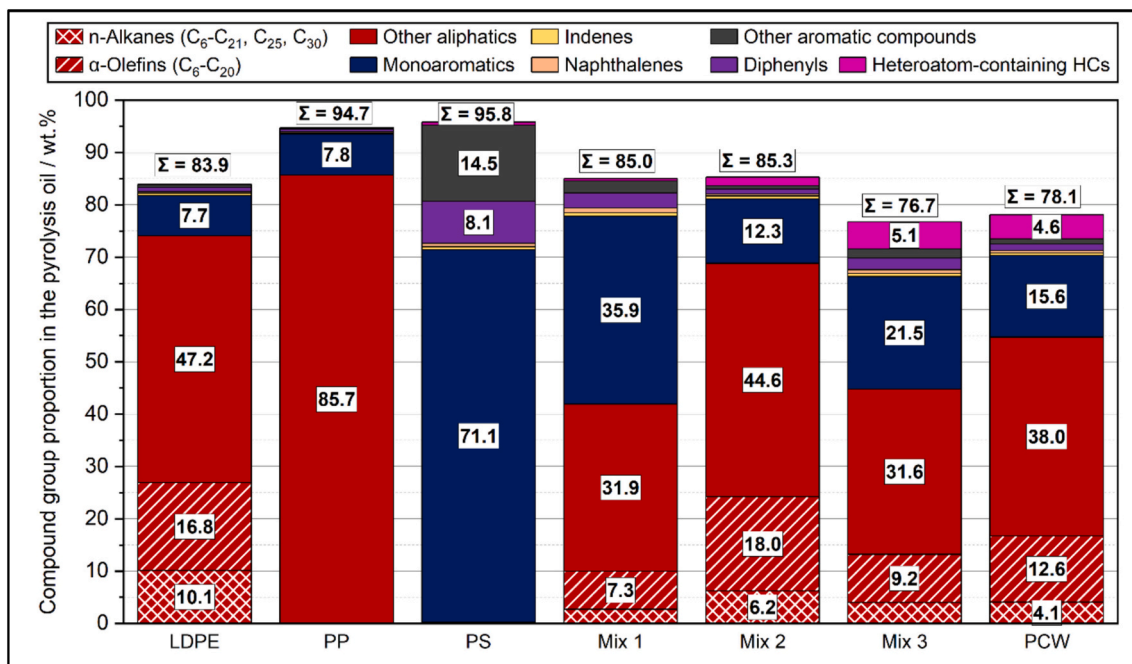


Fig. 7. Compound group-specific GC $\times$ GC results of the investigated pyrolysis oils stemming from different thermoplastic feedstocks pyrolyzed at 500 °C reactor set temperature in a screw reactor.

Errors originating from the integration methodology are considered relatively low in this approach. A key influencing factor is the boiling range of the pyrolysis oil under investigation. This is evidenced by higher losses in LDPE samples, likely due to high-boiling waxes and increased heteroatom content in the blends. The presence of heteroatoms promotes the formation of short-chain organic compounds, which may fall within the solvent range and are potentially discriminated because of reduced resolution in this range. Alternative solvents could potentially solve this issue. Commonly used solvents such as acetone, hexane, or isopropanol exhibit disadvantages, including overlap with other essential components or lower capability of solving all pyrolysis oil compounds. Therefore, carbon disulfide might be a potential solvent enhancing future analyses. Additionally, heteroatom-containing compounds may elute in other compound group retention time ranges. For benzoic acid, for example, the blob is quantifiable and was corrected by adding the volume to the group of heteroatom-containing HC and subtracting it from the monoaromatic range. Compounds of low content may not be unambiguously identified. In such cases, a compound group correction is not feasible. Furthermore, pyrolysis oil samples from PS and PCW demonstrate wrap-around effects in the second dimension, despite relatively long modulation times. Examples include  $\epsilon$ -caprolactam and styrene trimers. Particularly in pure PS samples, higher amounts of additional high-boiling components with increased wrap-around are observed. Without group range adaptation for PS, these would be incorrectly attributed to the aliphatic region. Therefore, the compound group range is adjusted for pure PS pyrolysis oils. For predominantly olefinic mixtures, this error is negligible due to the minimal PS content. In addition to the identified compound groups, repeating blobs are observed in the retention time window of approximately 40 to 70 min (first dimension) and 3 to 4 s (second dimension) in the blends and PCW. These are presumed to be increasingly long, unbranched aliphatic chains with a single functional group, potentially amines, alcohols, or phenyl-alkanes. Such species may form via gas-phase reactions of reactive primary products. Reliable identification would require higher mass spectrometric resolution, achievable by broadening the scan range to higher mass fractions, e.g. to 400 or 450 u. However, this adaptation could presumably lower the resolution in the chromatogram because of the extended cycle time. Alternatively, the implementation of a more advanced MS type, like a time-of-flight MS, rather than a quadrupole MS, could overcome this problem.

The compound group evaluation matches the findings concluded from the NMR analyses. However, a quantitative comparison between the mass-related compound group-specific GC $\times$ GC results and the molar distribution of functional groups from the NMR analysis is challenging. Two aspects prevent this comparison. Firstly, the structures within a group in GC $\times$ GC are diverse. Saturated or unsaturated substituents of varying chain lengths are often found on aromatics. For example, benzene, but partly pentyl-benzene, can be identified within the monoaromatic group. Simplifying the compound groups to a specific molar distribution fails to account for the diversity of different molecules within the compound group and substantially distorts the result. Second, the GC $\times$ GC method determines between 76 wt% and 96 wt% of the total mass. NMR always detects all functional groups. Accordingly, almost the entire sample is detected in some oil. In the case of PS, a calculation would therefore be possible except for the problem mentioned above. With 25 wt% of compounds not detected in the GC $\times$ GC, as in the case of the oil from Mix 2 and Mix 3, a significant distortion is to be expected. Consequently, a quantitative comparison is not feasible. The first barrier, in particular, but also the second one, prevents reasonable calculations. While GC $\times$ GC analysis offers a much more detailed evaluation, the analysis is still elaborate. In contrast, NMR analyses on a benchtop device offer a limited level of detail but are highly valuable for screening experiments thanks to their robustness, comparatively short analysis time, and fast data evaluation.

### 3.4.3. Measurement uncertainties and technical limitations

The GC $\times$ GC method is subject to statistical and systematic errors. Statistical errors can be estimated based on the deviation of the double measurement of the pyrolysis oils. Apart from negligible retention time shifts, the chromatograms are identical. These shifts result from modulation and do not influence the measurement result. They are corrected during data processing. Corresponding chromatograms of each pyrolysis oil show identical blobs with hardly any variation in blob volume. For main compound analysis, the statistical error is evaluated based on multiple compounds in different samples, e.g.,  $\alpha$ -decene and linear C<sub>20</sub> aliphatics in LDPE pyrolysis oil, styrene and 1,3-diphenylpropane in PS pyrolysis oil, and benzoic acid, acetophenone, and benzonitrile in the PCW pyrolysis oil. The statistical error, which could be attributed to measurement inaccuracies, e.g., during sampling or sample preparation, is low. The standard deviations depend on the compound and the sample under investigation. It accounts for less than 2.5 % compared to the average compound concentration. The maximum deviation is found for benzoic acid, which is expected, as this compound features significant tailing. Blobs with uniform shape feature a standard deviation of less than 1.2 %. This result emphasizes the reproducibility of the main compound quantification results obtained with this GC $\times$ GC method.

However, for compound group quantification, further systematic errors are possible. Uncertainties may arise from the assumed response factors. The compound group response factors reflect a reasonable average of factors calibrated for compounds in the corresponding retention time range. Yet, they may deviate from the individual response factors of the unknown components within the group. Depending on the sample composition, this can lead to discrimination in the form of overestimation or underestimation of compound group proportions. Offsetting the quantified main components in the compound group range significantly reduces this influence. The offset reduces the impact of errors caused when calculating the mass-related share of the group with the associated response factor, since it reduces the unidentified compound group volume. Nevertheless, this systematic error is considered to be more significant for the measurement uncertainty of the compound group quantification than statistical error. Furthermore, the technical limitations (e.g., incomplete evaporation of high-boiling species and overlapping blobs in the boiling range of C<sub>5</sub>–C<sub>6</sub> alkanes), which have already been discussed in the manuscript, are assumed to impact the quantitative compound group results more than the statistical errors. Therefore, when evaluating compound group quantification, it is important to consider the sum of all identified components and compare this with simulated distillation results. While the naphtha and middle distillate cut can be resolved well, the boiling range of VGO needs further analysis by high-temperature GC $\times$ GC.

## 4. Conclusion

The study highlights the importance of complementary analytical methods for the comprehensive characterization of pyrolysis oils from polyolefin-rich mixed plastics. In addition to commonly used elemental and one-dimensional gas chromatography, GC $\times$ GC methods must be employed for the holistic characterization of pyrolysis oils from thermoplastic feedstocks. Simulated distillation also provides key indicators for the subsequent reintegration of the condensable products into petrochemical processes.

A GC $\times$ GC method enabling the quantification of the most important main components, heteroatomic trace substances, and group-based evaluations has been developed. This method has been tailored to thermoplastic mixtures containing impurities of nitrogen, oxygen, and chlorine. It covers the most important HC groups forming in polyolefin and PS pyrolysis. Additionally, the extensive calibration and excellent blob separation enable the quantification of numerous heteroatom-containing products. The method allows for analyzing samples in a wide boiling range from naphtha to middle distillate, and with a complex composition of different compound groups. Furthermore, the



group-based evaluation enables a characterization of 77–95 wt% of the thermoplastics-based pyrolysis oils used in this study. The results are consistent with the decomposition mechanisms and product spectrum of thermoplastics reported in the literature. The identified products can be attributed to specific polymers in the mixture. Alongside benzoic acid,  $\epsilon$ -caprolactam, acetophenone, and aromatic nitriles, benzaldehydes and both, conjugated and non-conjugated polyaromatics were identified as main impurities for further pyrolysis oil processing. Their proportion of up to 9 wt% emphasizes the importance of further detailed analysis of compound groups despite paraffinic species.

The results confirm the applicability of the GC×GC method to mixtures of heteroatomic thermoplastics such as PET, PA6, PVC, and ABS with up to 25 wt%. This feedstock classification applies to most waste fractions from packaging sorting residues, automotive shredder residues, or commercial waste collections discussed for chemical recycling [54]. Using this method instead of a combination of different GC×GC setups with different element-specific detectors enables detailed characterization at lower investment costs and with less time expenditure. The implementation of the NCD represents a supplementary quantification option for nitrogen-containing compounds for future method optimization. Thus, the level of detail and robustness of the results could be further enhanced.

The presence of heteroatoms and complex aromatic compounds in pyrolysis oil poses a challenge to processing it within established polymer or chemical production pathways [9]. Thus, the combined analyses enable the reliable evaluation of pyrolysis oils concerning their suitability for reintegration into various large-scale chemical plants, especially crackers. Furthermore, the GC×GC method offers the potential to relate specific problematic compounds in the oil to distinct polymers in the feedstock or feedstock interactions. Combining standard chemical analyses with the novel GC×GC method allows for improving pyrolysis plants in terms of scale-up, reactor design, and process conditions. Further parameters, such as viscosity and density, must be checked for compliance with common specifications through additional analyses. For this, it is crucial to interpret the compound group analysis in relation to the elemental analyses, including the derived heteroatom content and H/C. NMR Analysis or further GC methods tailored to PIONA analysis are needed, as they can resolve the content of saturated and unsaturated compounds in more detail.

However, the analyses reveal the importance of upgrading pyrolysis oil for its use as a substitute feedstock in the chemical industry, given that nitrogen, oxygen, and chlorine content significantly exceed specification limits [9]. Thus, further upgrading of pyrolysis oil or dilution with fossil naphtha is required before pyrolysis oils can be used as feedstock for steam crackers. Alternatively, pyrolysis oil components need further separation to enrich compound groups in product fractions that fit reintegration pathways. The presented GC×GC method also emerges as an advanced analysis for suitability tests of such upgraded and fractionated pyrolysis oils intended for closing the polymer-to-polymer recycling circle.

#### CRediT authorship contribution statement

**Niklas Netsch:** Writing – original draft, Visualization, Validation, Software, Methodology, Formal analysis, Data curation, Conceptualization. **Luca Weigel:** Software, Methodology. **Tim Schmedding:** Methodology. **Michael Zeller:** Writing – review & editing, Methodology, Conceptualization. **Britta Bergfeldt:** Writing – review & editing, Resources, Formal analysis. **Grazyna Straczewski:** Writing – review & editing, Resources. **Salar Tavakkol:** Writing – review & editing, Supervision, Resources, Funding acquisition. **Dieter Stapf:** Writing – review & editing, Supervision, Resources, Funding acquisition.

#### Funding sources

Funding of this work was provided by the German Helmholtz

Association within the program Materials and Technologies for the Energy Transition (MTET).

#### Declaration of competing interest

The authors declare no competing financial interest.

#### Acknowledgment

The authors also gratefully acknowledge the support of Patrick Schieber and Aylin Hannemann in performing the supporting oil analysis.

#### Appendix A. Supplementary data

Supplementary data to this article can be found online at <https://doi.org/10.1016/j.fuproc.2025.108359>.

#### Data availability

Data will be made available on request.

#### References

- [1] M. Laghezza, S. Fiore, F. Berruti, A review on the pyrolytic conversion of plastic waste into fuels and chemicals, *J. Anal. Appl. Pyrolysis* 179 (2024) 106479, <https://doi.org/10.1016/j.jaap.2024.106479>.
- [2] S.H. Chang, Plastic waste as pyrolysis feedstock for plastic oil production: a review, *Sci. Total Environ.* 877 (2023) 162719, <https://doi.org/10.1016/j.scitotenv.2023.162719>.
- [3] L. Dai, N. Zhou, Y. Lv, Y. Cheng, Y. Wang, Y. Liu, K. Cobb, P. Chen, H. Lei, R. Ruan, Pyrolysis technology for plastic waste recycling: a state-of-the-art review, *Prog. Energy Combust. Sci.* 93 (2022) 101021, <https://doi.org/10.1016/j.peecs.2022.101021>.
- [4] G. Lopez, M. Artetxe, M. Amutio, J. Bilbao, M. Olazar, Thermochemical routes for the valorization of waste polyolefinic plastics to produce fuels and chemicals. A review, *Renew. Sust. Energ. Rev.* 73 (2017) 346–368, <https://doi.org/10.1016/j.rser.2017.01.142>.
- [5] M. Kusenberg, A. Eschenbacher, L. Delva, S. de Meester, E. Delikonstantis, G. D. Stefanidis, K. Ragaert, K.M. van Geem, Towards high-quality petrochemical feedstocks from mixed plastic packaging waste via advanced recycling: the past, present and future, *Fuel Process. Technol.* 238 (2022) 107474, <https://doi.org/10.1016/j.fuproc.2022.107474>.
- [6] E. Rodríguez, A. Gutiérrez, R. Palos, F.J. Vela, J.M. Arandes, J. Bilbao, Fuel production by cracking of polyolefins pyrolysis waxes under fluid catalytic cracking (FCC) operating conditions, *Waste Manag.* 93 (2019) 162–172, <https://doi.org/10.1016/j.wasman.2019.05.005>.
- [7] R. Palos, A. Gutiérrez, F.J. Vela, J.A. Maña, I. Hita, A. Asueta, S. Arnaiz, J. M. Arandes, J. Bilbao, Assessing the potential of the recycled plastic slow pyrolysis for the production of streams attractive for refineries, *J. Anal. Appl. Pyrolysis* 142 (2019) 104668, <https://doi.org/10.1016/j.jaap.2019.104668>.
- [8] C.S. Hsu, P.R. Robinson, *Springer Handbook of Petroleum Technology*, second ed., Springer International Publishing, Cham, 2017.
- [9] M. Kusenberg, A. Eschenbacher, M.R. Djokic, A. Zayoud, K. Ragaert, S. de Meester, K.M. van Geem, Opportunities and challenges for the application of post-consumer plastic waste pyrolysis oils as steam cracker feedstocks: to decontaminate or not to decontaminate? *Waste Manag.* 138 (2022) 83–115, <https://doi.org/10.1016/j.wasman.2021.11.009>.
- [10] E. Hoekstra, S.R. Kersten, A. Tudos, D. Meier, K.J. Hogendoorn, Possibilities and pitfalls in analyzing (upgraded) pyrolysis oil by size exclusion chromatography (SEC), *J. Anal. Appl. Pyrolysis* 91 (2011) 76–88, <https://doi.org/10.1016/j.jaap.2011.01.006>.
- [11] E.A. Williams, P.T. Williams, The pyrolysis of individual plastics and a plastic mixture in a fixed bed reactor, *J. Chem. Technol. Biotechnol.* 70 (1997) 9–20, [https://doi.org/10.1002/\(SICI\)1097-4660\(199709\)70:1<9::AID-JCTB700>3.0.CO;2-E](https://doi.org/10.1002/(SICI)1097-4660(199709)70:1<9::AID-JCTB700>3.0.CO;2-E).
- [12] N. Hao, H. Ben, C.G. Yoo, S. Adhikari, A.J. Ragauskas, Review of NMR characterization of pyrolysis oils, *Energy Fuel* 30 (2016) 6863–6880, <https://doi.org/10.1021/acs.energyfuels.6b01002>.
- [13] U. Kumar, V. Gaikwad, M. Mayyas, M. Bucknall, V. Sahajwalla, Application of high-resolution NMR and GC-MS to study hydrocarbon oils derived from noncatalytic thermal transformation of e-waste plastics, *ACS Omega* 3 (2018) 9282–9289, <https://doi.org/10.1021/acsomega.8b01284>.
- [14] P.T. Williams, E.A. Williams, Interaction of plastics in mixed-plastics pyrolysis, *Energy Fuel* 13 (1999) 188–196, <https://doi.org/10.1021/ef980163x>.
- [15] R.L. Ware, S.M. Rowland, R.P. Rodgers, A.G. Marshall, Advanced Chemical characterization of pyrolysis oils from landfill waste, recycled plastics, and forestry residue, *Energy Fuel* 31 (2017) 8210–8216, <https://doi.org/10.1021/acs.energyfuels.7b00865>.

- [16] B. Diehl, G. Randel, Analysis of biodiesel, diesel and gasoline by NMR spectroscopy – a quick and robust alternative to NIR and GC, *Lipid Technol.* 19 (2007) 258–260, <https://doi.org/10.1002/lite.200700087>.
- [17] C. Mase, J.F. Maillard, B. Paupy, M. Farenc, C. Adam, M. Hubert-Roux, C. Afonso, P. Giusti, Molecular characterization of a mixed plastic pyrolysis oil from municipal wastes by direct infusion fourier transform ion cyclotron resonance mass spectrometry, *Energy Fuel* 35 (2021) 14828–14837, <https://doi.org/10.1021/acs.energyfuels.1c01678>.
- [18] T. Maqsood, J. Dai, Y. Zhang, M. Guang, B. Li, Pyrolysis of plastic species: a review of resources and products, *J. Anal. Appl. Pyrolysis* 159 (2021) 105295, <https://doi.org/10.1016/j.jaap.2021.105295>.
- [19] W. Kaminsky, J.-S. Kim, Pyrolysis of mixed plastics into aromatics, *J. Anal. Appl. Pyrolysis* 51 (1999) 127–134, [https://doi.org/10.1016/S0165-2370\(99\)00012-1](https://doi.org/10.1016/S0165-2370(99)00012-1).
- [20] N. Hassibi, Y. Quiring, V. Carré, F. Aubriet, L. Vernex-Loiset, G. Mauviel, V. Burklé-Vitzthum, Analysis and control of products obtained from pyrolysis of polypropylene using a reflux semi-batch reactor and GC-MS/FID and FT-ICR MS, *J. Anal. Appl. Pyrolysis* 169 (2023) 105826, <https://doi.org/10.1016/j.jaap.2022.105826>.
- [21] N. Netsch, M. Simons, A. Feil, H. Leibold, F. Richter, J. Slama, S.P. Yogish, K. Greiff, D. Stapf, Recycling of polystyrene-based external thermal insulation composite systems - application of combined mechanical and chemical recycling, *Waste Manag.* 150 (2022) 141–150, <https://doi.org/10.1016/j.wasman.2022.07.001>.
- [22] M.S. Abbas-Abadi, M.N. Haghighi, H. Yeganeh, Evaluation of pyrolysis product of virgin high density polyethylene degradation using different process parameters in a stirred reactor, *Fuel Process. Technol.* 109 (2013) 90–95, <https://doi.org/10.1016/j.fuproc.2012.09.042>.
- [23] B.A. Perez, J.V.J. Krishna, H.E. Toraman, Characterization of polyolefins-based pyrolysis oils: a comparison between one-dimensional gas chromatography and two-dimensional gas chromatography, *J. Chromatogr.* 1739 (2025) 465510, <https://doi.org/10.1016/j.chroma.2024.465510>.
- [24] T. Dutriez, M. Courtiade, D. Thiébaud, H. Dulot, M.-C. Hennion, Improved hydrocarbons analysis of heavy petroleum fractions by high temperature comprehensive two-dimensional gas chromatography, *Fuel* 89 (2010) 2338–2345, <https://doi.org/10.1016/j.fuel.2009.11.041>.
- [25] T. Dijkmans, K.M. van Geem, M.R. Djokic, G.B. Marin, Combined comprehensive two-dimensional gas chromatography analysis of polyaromatic hydrocarbons/polyaromatic sulfur-containing hydrocarbons (PAH/PASH) in complex matrices, *Ind. Eng. Chem. Res.* 53 (2014) 15436–15446, <https://doi.org/10.1021/ie5000888>.
- [26] M.R. Djokic, H. Muller, N.D. Ristic, A.R. Akhras, S.H. Symoens, G.B. Marin, K. M. van Geem, Combined characterization using HT-GC × GC-FID and FT-ICR MS: a pyrolysis fuel oil case study, *Fuel Process. Technol.* 182 (2018) 15–25, <https://doi.org/10.1016/j.fuproc.2018.10.007>.
- [27] M.E. Machado, Comprehensive two-dimensional gas chromatography for the analysis of nitrogen-containing compounds in fossil fuels: a review, *Talanta* 198 (2019) 263–276, <https://doi.org/10.1016/j.talanta.2019.02.031>.
- [28] T. Sfetsas, C. Michailof, A. Lappas, Q. Li, B. Kneale, Qualitative and quantitative analysis of pyrolysis oil by gas chromatography with flame ionization detection and comprehensive two-dimensional gas chromatography with time-of-flight mass spectrometry, *J. Chromatogr. A* 1218 (2011) 3317–3325, <https://doi.org/10.1016/j.chroma.2010.10.034>.
- [29] M.S. Abbas-Abadi, M. Kusenber, A. Zayoud, M. Roosen, F. Vermeire, S. Madanikashani, M. Kuzmanović, B. Parvizi, U. Kresovic, S. de Meester, K.M. van Geem, Thermal pyrolysis of waste versus virgin polyolefin feedstocks: the role of pressure, temperature and waste composition, *Waste Manag.* 165 (2023) 108–118, <https://doi.org/10.1016/j.wasman.2023.04.029>.
- [30] H.E. Toraman, T. Dijkmans, M.R. Djokic, K.M. van Geem, G.B. Marin, Detailed compositional characterization of plastic waste pyrolysis oil by comprehensive two-dimensional gas-chromatography coupled to multiple detectors, *J. Chrom. A* 1359 (2014) 237–246, <https://doi.org/10.1016/j.chroma.2014.07.017>.
- [31] M.S. Abbas-Abadi, A. Zayoud, M. Kusenber, M. Roosen, F. Vermeire, P. Yazdani, J. van Waeyenberg, A. Eschenbacher, F.J.A. Hernandez, M. Kuzmanović, H. Dao Thi, U. Kresovic, B. Sels, P. van Puyvelde, S. de Meester, M. Saeys, K.M. van Geem, Thermochemical recycling of end-of-life and virgin HDPE: a pilot-scale study, *J. Anal. Appl. Pyrolysis* 166 (2022) 105614, <https://doi.org/10.1016/j.jaap.2022.105614>.
- [32] M. Kusenber, A. Zayoud, M. Roosen, H.D. Thi, M.S. Abbas-Abadi, A. Eschenbacher, U. Kresovic, S. de Meester, K.M. van Geem, A comprehensive experimental investigation of plastic waste pyrolysis oil quality and its dependence on the plastic waste composition, *Fuel Process. Technol.* 227 (2022) 107090, <https://doi.org/10.1016/j.fuproc.2021.107090>.
- [33] R.L. Ware, S.M. Rowland, J. Lu, R.P. Rodgers, A.G. Marshall, Compositional and structural analysis of silica gel fractions from municipal waste pyrolysis oils, *Energy Fuel* 32 (2018) 7752–7761, <https://doi.org/10.1021/acs.energyfuels.8b00596>.
- [34] H. Dao Thi, M.R. Djokic, K.M. van Geem, Detailed group-type characterization of plastic-waste pyrolysis oils: by comprehensive two-dimensional gas chromatography including linear, branched, and di-olefins, *Separations* 8 (2021) 103, <https://doi.org/10.3390/separations8070103>.
- [35] M. Beccaria, M. Piparo, Y. Zou, P.-H. Stefanuto, G. Purcaro, A.L. Mendes Siqueira, A. Maniquet, P. Giusti, J.-F., Focant, Analysis of mixed plastic pyrolysis oil by comprehensive two-dimensional gas chromatography coupled with low- and high-resolution time-of-flight mass spectrometry with the support of soft ionization, *Talanta* 252 (2023) 123799, <https://doi.org/10.1016/j.talanta.2022.123799>.
- [36] H.C. Genuino, M.C.P. van Eijk, S.R.A. Kersten, M.P. Ruiz, Pyrolysis of real packaging plastic waste streams in a fluidized-bed pilot plant, *Energy Fuel* (2025), <https://doi.org/10.1021/acs.energyfuels.3c04114>.
- [37] E. Lazzari, M. Piparo, C. Mase, L. Levacher, P.-H. Stefanuto, G. Purcaro, J.-F. Focant, P. Giusti, Chemical elucidation of recycled plastic pyrolysis oils by means of GC×GC-PI-TOF-MS and GC-VUV, *J. Anal. Appl. Pyrolysis* 176 (2023) 106224, <https://doi.org/10.1016/j.jaap.2023.106224>.
- [38] A. Eschenbacher, R.J. Varghese, J. Weng, K.M. van Geem, Fast pyrolysis of polyurethanes and polyisocyanurate with and without flame retardant: Compounds of interest for chemical recycling, *J. Anal. Appl. Pyrolysis* 160 (2021) 105374, <https://doi.org/10.1016/j.jaap.2021.105374>.
- [39] A. Jean, B.C. Magalhaes, P. Pijcke, N. Verhoosel, T. Sanliturk, Y. Ureel, M. Kusenber, M. Ruitenbeek, G. Bellos, K.M. van Geem, M.N. Dunkle, Organochloride speciation in plastic pyrolysis oil by GC × GC coupled to high-resolution TOF-MS using scripting expressions, *Anal. Chem.* 97 (2025) 10680–10690, <https://doi.org/10.1021/acs.analchem.5c00546>.
- [40] B.A. Perez, H.E. Toraman, Investigating primary decomposition of polypropylene through detailed compositional analysis using two-dimensional gas chromatography and principal component analysis, *J. Anal. Appl. Pyrolysis* 177 (2024) 106376, <https://doi.org/10.1016/j.jaap.2024.106376>.
- [41] C. Kibuta, O. Akin, D. Withoeck, Q. He, M. Schmidt, R.J. Varghese, M. Schlummer, S. de Meester, F.D. Calik, M. Denton, A. Buettner, K.M. van Geem, Assessing the feasibility of ocean plastic waste as secondary feedstock for the production of base chemicals, *Waste Manag.* 195 (2025) 167–176, <https://doi.org/10.1016/j.wasman.2025.02.003>.
- [42] N. Netsch, M. Zeller, F. Richter, B. Bergfeldt, S. Tavakkol, D. Stapf, Energy demand for pyrolysis of mixed thermoplastics and waste plastics in chemical recycling: model prediction and pilot-scale validation, *ACS Sustain. Resour. Manag.* 1 (2024) 1485–1492, <https://doi.org/10.1021/acssusresmg.4c00109>.
- [43] J. Vogt, A.D. Renno, M. Fuchs, T. Kurtz, N. Netsch, F. Richter, G. Straczewski, B. Bergfeldt, Y.C. Madriz-Diaz, A.D.L. Ribeiro, D. Ebert, S. Tavakkol, S. Raatz, D. Stapf, Chemical recycling of refrigerator plastic waste by pyrolysis: yields, product composition, and potential applications, *Fuel* 400 (2025) 135776, <https://doi.org/10.1016/j.fuel.2025.135776>.
- [44] H. Bockhorn, A. Hornung, U. Hornung, D. Schwallier, Kinetic study on the thermal degradation of polypropylene and polyethylene, *J. Anal. Appl. Pyrolysis* 48 (1999) 93–109, [https://doi.org/10.1016/S0165-2370\(98\)00131-4](https://doi.org/10.1016/S0165-2370(98)00131-4).
- [45] D.A. Skoog, F.J. Holler, S.R. Crouch, *Principles of Instrumental Analysis*, Sixth ed., Thomson Brooks/Cole, Belmont, 2007.
- [46] T. Faravelli, M. Pincioli, F. Pisano, G. Bozzano, M. Dente, E. Ranzi, Thermal degradation of polystyrene, *J. Anal. Appl. Pyrolysis* 60 (2001) 103–121, [https://doi.org/10.1016/S0165-2370\(00\)00159-5](https://doi.org/10.1016/S0165-2370(00)00159-5).
- [47] G. Montaudo, C. Puglisi, F. Samperi, Primary thermal degradation mechanisms of PET and PBT, *Polym. Degrad. Stab.* 42 (1993) 13–28, [https://doi.org/10.1016/0141-3910\(93\)90021-A](https://doi.org/10.1016/0141-3910(93)90021-A).
- [48] J. Yu, L. Sun, C. Ma, Y. Qiao, H. Yao, Thermal degradation of PVC: a review, *Waste Manag.* 48 (2016) 300–314, <https://doi.org/10.1016/j.wasman.2015.11.041>.
- [49] K.-H. Lee, D.-H. Shin, Y.-H. Seo, Thermal degradation of nitrogen-containing polymers, acrylonitrile-butadiene-styrene and styrene-acrylonitrile, *Korean J. Chem. Eng.* 23 (2006) 224–229, <https://doi.org/10.1007/BF02705720>.
- [50] M. Holtkamp, M. Renner, K. Matthiesen, M. Wald, G.A. Luinstra, P. Biessey, Robust downstream technologies in polystyrene waste pyrolysis: design and prospective life-cycle assessment of pyrolysis oil reintegration pathways, *Resour. Conserv. Recycl.* 205 (2024) 107558, <https://doi.org/10.1016/j.resconrec.2024.107558>.
- [51] J. Yang, Y. Wu, J. Zhu, H. Yang, Y. Li, L. Jin, H. Hu, Insight into the pyrolysis behavior of polyvinyl chloride using in situ pyrolysis time-of-flight mass spectrometry: Aromatization mechanism and Cl evolution, *Fuel* 331 (2023) 125994, <https://doi.org/10.1016/j.fuel.2022.125994>.
- [52] B. Gui, Y. Qiao, D. Wan, S. Liu, Z. Han, H. Yao, M. Xu, Nascent tar formation during polyvinylchloride (PVC) pyrolysis, *Proc. Combust. Inst.* 34 (2013) 2321–2329, <https://doi.org/10.1016/j.proci.2012.08.013>.
- [53] R. Cao, M.Q. Zhang, Y. Jiao, B. Sun, D. Xiao, M. Wang, D. Ma, Co-upcycling of polyvinyl chloride and polyesters, *Nat. Sustain.* 6 (2023) 1685–1692, <https://doi.org/10.1038/s41893-023-01234-1>.
- [54] M. Zeller, N. Netsch, F. Richter, H. Leibold, D. Stapf, Chemical recycling of mixed plastic wastes by pyrolysis – pilot scale investigations, *Chem. Ing. Tech.* 93 (2021) 1763–1770, <https://doi.org/10.1002/cite.202100102>.